J|A|C|S
ARTICLES
Published on Web 08/29/2006

# Unusual Hydrogen Bonding in Water-Filled Carbon Nanotubes

Oleg Byl,[†] Jin-Chen Liu,[†,‡] Yang Wang,[‡] Wai-Leung Yim,[§] J. Karl Johnson,[‡,||] and John T. Yates, Jr.*[,†]

*Contributions from the Department of Chemistry, Surface Science Center, University of Pittsburgh, Pittsburgh, Pennsylvania 15260, Department of Chemical Engineering, University of Pittsburgh, Pittsburgh, Pennsylvania 15261, Oldenburg Institut fur Reine und Angewandte Chemie, Carl von Ossietzky Universität, Carl-von-Ossietzky Str. 9-11, 26129 Oldenburg, Germany, and National Energy Technology Laboratory, Pittsburgh, Pennsylvania 15236*

Received November 18, 2005; E-mail: jyates@pitt.edu

***Abstract:*** We present the first experimental vibrational spectroscopy study providing direct evidence of a water phase inside single-walled carbon nanotubes that exhibits an unusual form of hydrogen-bonding due to confinement. Water adopts a stacked-ring structure inside nanotubes, forming intra- and inter-ring hydrogen bonds. The intra-ring hydrogen bonds are bulk-like while the inter-ring hydrogen bonds are relatively weak, having a distorted geometry that gives rise to a distinct OH stretching mode. The experimentally observed infrared mode at 3507 $cm^{-1}$ is assigned to vibrations of the inter-ring OH-groups based on detailed atomic-level modeling. The direct observation of unusual hydrogen bonding in nanotubes has potential implications for water in other highly confined systems, such as biological channels and nanoporous media.

## Introduction

Confined matter on the nanometer scale differs significantly from bulk matter.[1] Widespread interest exists in the structure of confined water,[2−11] in its degree of hydrogen bonding,[7,12−16] and in proton transfer through "water wires".[17,18] The special properties of confined water can influence molecular transport inside membrane pores.[19,20]

Confinement of water can be reached by limiting the size of water agglomerates in one, two, or three dimensions. In an infinite ice crystal each water molecule, complying with the "bulk ice rule",[2] is tetrahedrally coordinated, simultaneously donating and accepting two hydrogen atoms, forming a hydrogen-bonded network. However this arrangement is disrupted in agglomerates of crystalline water of finite sizes, leading to a variety of shapes for small water clusters with different types of OH groups ranging from bulk-like to essentially free OH groups. This diversity can be readily detected by means of vibrational spectroscopy that provides one of the most insightful means for OH characterization.[21]

A number of experimental vibrational spectroscopy studies of water clusters with sizes ranging from a few molecule agglomerates[22−24] to hundred- and thousand-molecule clusters[25] to macroscopic crystals[26−28] show that four major types of OH stretching modes can be detected for water structures with reduced dimensionality. These modes originate from the OH groups that belong to the following water species (spectral regions given in parentheses): "free OH" groups dangling from the surface (3690−3720 $cm^{-1}$), double H-atom donor−single

[†] Department of Chemistry, University of Pittsburgh.
[‡] Department of Chemical Engineering, University of Pittsburgh.
[§] Carl von Ossietzky Universität
[||] National Energy Technology Laboratory.

(1) Gelb, L. D.; Gubbins, K. E.; Radhakrishnan, R.; Sliwinska-Bartkowiak, M. *Rep. Prog. Phys.* **1999**, *62*, 1573.
(2) Buch, V.; Devlin, J. P. *Water in Confining Geometries*; Springer: Berlin, New York, 2003.
(3) Koga, K.; Gao, G. T.; Tanaka, H.; Zeng, X. C. *Nature* **2001**, *412*, 802.
(4) Hummer, G.; Rasaiah, J. C.; Noworyta, J. P. *Nature* **2001**, *414*, 188.
(5) Noon, W. H.; Ausman, K. D.; Smalley, R. E.; Ma, J. P. *Chem. Phys. Lett.* **2002**, *355*, 445.
(6) Kolesnikov, A. I.; Zanotti, J. M.; Loong, C. K.; Thiyagarajan, P.; Moravsky, A. P.; Loutfy, R. O.; Burnham, C. J. *Phys. Rev. Lett.* **2004**, *93*, 035503.
(7) Mashl, R. J.; Joseph, S.; Aluru, N. R.; Jakobsson, E. *Nano Lett.* **2003**, *3*, 589.
(8) Tanaka, H.; Koga, K. In *Water in Confining Geometries*; Buch, V., Devlin, J. P., Eds.; Springer: Berlin; New York, 2003; p 151.
(9) Bellissent-Funel, M. C. *Eur. Phys. J. E.* **2003**, *12*, 83.
(10) Maniwa, Y.; Kataura, H.; Abe, M.; Suzuki, S.; Achiba, Y.; Kira, H.; Matsuda, K. *J. Phys. Soc. Jpn.* **2002**, *71*, 2863.
(11) Maniwa, Y.; Kataura, H.; Abe, M.; Udaka, A.; Suzuki, S.; Achiba, Y.; Kira, H.; Matsuda, K.; Kadowaki, H.; Okabe, Y. *Chem. Phys. Lett.* **2005**, *401*, 534.
(12) Gordillo, M. C.; Martí, J. *Chem. Phys. Lett.* **2000**, *329*, 341.
(13) Wang, J.; Zhu, Y.; Zhou, J.; Lu, X. H. *Phys. Chem. Chem. Phys.* **2004**, *6*, 829.
(14) Martí, J.; Gordillo, M. C. *Chem. Phys. Lett.* **2002**, *354*, 227.
(15) Gordillo, M. C.; Martí, J. *Chem. Phys. Lett.* **2001**, *341*, 250.
(16) Marti, J.; Gordillo, M. C. *Phys. Rev. B* **2001**, *63*, 165430.
(17) Mann, D. J.; Halls, M. D. *Phys. Rev. Lett.* **2003**, *90*, 195503.
(18) Dellago, C.; Naor, M. M.; Hummer, G. *Phys. Rev. Lett.* **2003**, *91*, 105902.
(19) Levinger, N. E. *Science* **2002**, *298*, 1722.
(20) Yui, H.; Guo, Y.; Koyama, K.; Sawada, T.; John, G.; Yang, B.; Masuda, M.; Shimizu, T. *Langmuir* **2005**, *21*, 721.
(21) Pimentel, G. C.; McClellan, A. L. *The Hydrogen Bond*; W.H. Freeman: San Francisco, 1960.
(22) Gruenloh, C. J.; Carney, J. R.; Arrington, C. A.; Zwier, T. S.; Fredericks, S. Y.; Jordan, K. D. *Science* **1997**, *276*, 1678.
(23) Pribble, R. N.; Zwier, T. S. *Faraday Discuss.* **1994**, *229*.
(24) Pribble, R. N.; Zwier, T. S. *Science* **1994**, *265*, 75.
(25) Andersson, P.; Steinbach, C.; Buck, U. *Eur. Phys. J. D.* **2003**, *24*, 53.
(26) Devlin, J. P.; Buch, V. *J. Phys. Chem.* **1995**, *99*, 16534.
(27) Rowland, B.; Kadagathur, N. S.; Devlin, J. P.; Buch, V.; Feldman, T.; Wojcik, M. J. *J. Chem. Phys.* **1995**, *102*, 8328.
(28) Devlin, J. P.; Buch, V. *J. Phys. Chem. B.* **1997**, *101*, 6095.

10.1021/ja057856u CCC: $33.50 

O-atom acceptor (~3450−3550 $cm^{-1}$), water molecules in a distorted tetragonal coordination (~3400−3450 $cm^{-1}$), and single donor−double acceptor (3050−3200 $cm^{-1}$). The position of the OH stretching mode points to the degree of involvement of the OH group into the hydrogen-bond network. Studies of the ice surface show that water molecules tend to rearrange into surface ring structures to reduce the number of free OH groups.[26−28]

In accord with experimental studies, theoretical calculations on water clusters indicate that water agglomerates can be stabilized by minimization of the number of free OH groups.[22,29−32] This occurs by formation of rings composed of hydrogen-bonded $H_2O$ molecules. Thus, a water cluster may have several rings of different sizes that can be irregularly oriented with respect to each other. Some computations show that the structures with water rings stacked on top of each other are one of the most stable. However, experimental verification of this can be complicated by the larger number of possible cluster shapes with an increasing number of water molecules in the cluster.

Single-walled carbon nanotubes have been shown to be a useful material for investigation of confinement effects.[33−38] They possess a deep van der Waals adsorption potential well in the interior. Quasi-one-dimensional conditions can be realized in the nanotube, thanks to their macroscopic lengths and diameters of about 1 nm. The nanotube interior is an ideal medium for the study of the hydrogen-bond network under extreme conditions, since a nanotube can provide a confining geometry without a strong interaction with $H_2O$ molecules, which may influence the hydrogen bonding.

Molecular dynamics calculations indicate that water confined in nanotubes less than 2 nm in diameter forms *n*-gonal structures formed of stacked rings at temperatures below ~280 K and pressures above 50 MPa.[3,8,39−41] Each ring consists of $n H_2O$ molecules ($n = 4-6$, depending on the nanotube diameter) with one OH group lying in the ring plane and the other oriented perpendicular to it. In this case, each water molecule (except those in the edge rings) in these phases is four-coordinated, i.e., each satisfies the bulk ice rule. At higher temperatures, two water phases have been predicted for nanotubes with diameters larger than 1.26 nm, namely the wall phase and the axial phase. The axial phase disappears upon cooling, causing a discontinuous liquid−solid phase transition.[6]

These predictions have been verified experimentally by X-ray diffraction,[10,11] NMR,[42] and neutron diffraction[6] studies. The most recent X-ray diffraction study of nanotube samples, with different average diameters, confirmed the dependence of the number of water molecules in a ring on the nanotube diameter.[11] The NMR study has shown that a liquid-to-solid transition for water confined in nanotubes proceeds in two steps: the axial phase freezes first, followed by solidification of the wall phase. A vibrational spectrum of water confined in carbon nanotubes has been studied by means of inelastic neutron scattering.[6] It was shown that the OH stretching mode of the confined water shifts to higher frequencies relative to the bulk ice. This shift has been attributed to weakening of the hydrogen bonds due to formation of *n*-gonal $H_2O$ structures inside nanotubes.

The strength of hydrogen bonds in *n*-gonal water structures (for $n = 5, 6$) confined in the nanotube interior has been studied by ab initio methods.[41] Theoretical predictions indicate that in the pentagonal water structure the axial (inter-ring) hydrogen bond should be weaker than the in-plane (intra-ring) hydrogen bond. This prediction is based on density functional theory calculations of the effective charges on the atoms and on calculated charge densities. The nonequivalency of two hydrogen bonds should lead to two different vibrational features and can be detected by means of IR spectroscopy.

To-date there has not been any direct experimental confirmation of the predicted weaker hydrogen bonds for water confined in single-walled carbon nanotubes (SWNTs). In this work, we report the first observation of a distinct sharp vibrational mode at 3507 $cm^{-1}$ that is unambiguously associated with a distorted hydrogen bond for water inside nanotubes. The location of the water molecules is determined by studying the effect of blocking the nanotube interior with *n*-nonane causing the 3507 $cm^{-1}$ band to be absent when water is adsorbed on the nanotubes. Our calculations are the first to directly link the structure of the water inside the nanotubes to the specific vibrational feature observed at 3507 $cm^{-1}$, predicted from both ab initio and classical simulations. We therefore demonstrate that vibrational spectroscopy, coupled with detailed molecular modeling, can be used as a sensitive probe of changes in hydrogen bonding due to confinement. This methodology may prove useful for investigating water in other highly confined environments.

## Experimental Section

The nanotubes were obtained from Prof. Smalley's group and were used in our previous studies.[34,35,43−46] Nanotubes were deposited directly onto a tungsten grid, which was inserted into a vacuum-IR cell.[34,47] This configuration causes the axis of each nanotube to lie in a plane roughly perpendicular to the direction of the incident IR beam. Opening of the nanotubes by ozonation was carried out in two 5-min cycles with 17.2/18.1 Torr and 17.3/18.2 Torr initial/final $O_3$ pressures, respectively.[34,35,48,49] The nanotubes were then annealed at 873 K for 30 min to remove the functionalities formed during the ozonation procedure. The resulting opening of the nanotubes was tested by $CF_4$ adsorption before and after the etching.[34]


(29) Tsai, C. J.; Jordan, K. D. *J. Phys. Chem.* **1993**, *97*, 5208.
(30) Lee, H. M.; Suh, S. B.; Kim, K. S. *J. Chem. Phys.* **2001**, *114*, 10749.
(31) Fanourgakis, G. S.; Apra, E.; de Jong, W. A.; Xantheas, S. S. *J. Chem. Phys.* **2005**, *122*, 134304.
(32) Lagutschenkov, A.; Fanourgakis, G. S.; Niedner-Schatteburg, G.; Xantheas, S. S. *J. Chem. Phys.* **2005**, *122*, 194310.
(33) Stan, G.; Cole, M. W. *Surf. Sci.* **1998**, *395*, 280.
(34) Byl, O.; Kondratyuk, P.; Forth, S. T.; FitzGerald, S. A.; Chen, L.; Johnson, J. K.; Yates, J. T., Jr. *J. Am. Chem. Soc.* **2003**, *125*, 5889.
(35) Byl, O.; Kondratyuk, P.; Yates, J. T., Jr. *J. Phys. Chem. B.* **2003**, *107*, 4277.
(36) Yim, W. L.; Byl, O.; Yates, J. T., Jr.; Johnson, J. K. *J. Am. Chem. Soc.* **2005**, *129*, 3198.
(37) Kuznetsova, A.; Yates, J. T., Jr.; Liu, J.; Smalley, R. E. *J. Chem. Phys.* **2000**, *112*, 9590.
(38) Simonyan, V. V.; Johnson, J. K.; Kuznetsova, A.; Yates, J. T. *J. Chem. Phys.* **2001**, *114*, 4180.
(39) Koga, K.; Parra, R. D.; Tanaka, H.; Zeng, X. C. *J. Chem. Phys.* **2000**, *113*, 5037.
(40) Koga, K.; Gao, G. T.; Tanaka, H.; Zeng, X. C. *Physica A* **2002**, *314*, 462.
(41) Bai, J.; Su, C. R.; Parra, R. D.; Zeng, X. C.; Tanaka, H.; Koga, K.; Li, J. M. *J. Chem. Phys.* **2003**, *118*, 3913.
(42) Ghosh, S.; Ramanathan, K. V.; Sood, A. K. *Europhys. Lett.* **2004**, *65*, 678.
(43) Yim, W. L.; Byl, O.; Yates, J. T., Jr.; Johnson, J. K. *J. Chem. Phys.* **2004**, *120*, 5377.
(44) Kondratyuk, P.; Wang, Y.; Johnson, J. K.; Yates, J. T., Jr. *J. Phys. Chem. B.* **2005**, *109*, 20999.
(45) Kondratyuk, P.; Yates, J. T., Jr. *Chem. Phys. Lett.* **2004**, *383*, 314.
(46) Kondratyuk, P.; Yates, J. T., Jr. *Chem. Phys. Lett.* **2005**, *410*, 324.
(47) Basu, P.; Ballinger, T. H.; Yates, J. T., Jr. *Rev. Sci. Instrum.* **1988**, *59*, 1321.
(48) Kuznetsova, A.; Yates, J. T., Jr.; Simonyan, V. V.; Johnson, J. K.; Huffman, C. B.; Smalley, R. E. *J. Chem. Phys.* **2001**, *115*, 6691.
(49) Mawhinney, D. B.; Naumenko, V.; Kuznetsova, A.; Yates, J. T., Jr.; Liu, J.; Smalley, R. E. *J. Am. Chem. Soc.* **2000**, *122*, 2383.

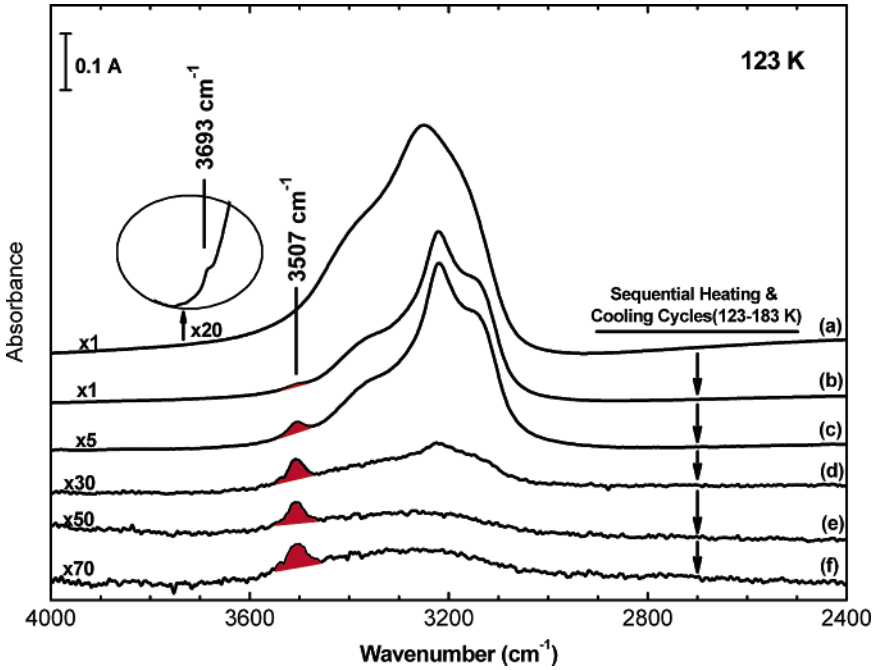


***Figure 1.*** Changes in the IR spectra of $H_2O$ condensed on single-walled carbon nanotubes on heating in a vacuum.

The experiment involving $H_2O$ diffusion into the nanotube interior was carried out as follows: (1) Water vapor was condensed to form amorphous ice on the outer geometric surface of the nanotubes at 123 K. Diffusion of water into the interior of the nanotubes is severely kinetically restricted at this temperature. (2) After the deposition and condensation, the sample was heated to 183 K and immediately quenched back to 123 K at a rate (in both directions) of 1 K/s. (3) Consecutive annealing and cooling cycles led to gradual removal into vacuum of both condensed ice and water adsorbed inside the nanotubes. A series of spectra for five heating/cooling cycles is shown in Figure 1; it is observed that a monotonic increase occurs in the ratio of the singular OH absorbance at 3507 $cm^{-1}$ to the integrated associated OH absorbance at lower frequencies as the coverage of water decreases.

Liquid He was used to decrease the sample temperatures for testing $H_2O$ diffusion inside nanotubes at very low coverages. The sample temperature was set within the range of 30−45 K and a small amount of $H_2O$ was dosed. Then the sample was heated to 153 K and cooled back to the initial temperature with a 1 K/s rate in both directions. Infrared spectra were measured before and after the heating. Figure 2 clearly shows the absence of the 3507 $cm^{-1}$ mode before annealing, followed by its appearance as $H_2O$ mobility occurs upon increasing the temperature.

To probe the internally bound water we utilized adsorbed *n*-nonane to block interior sites in the SWNTs. Figure 3 shows pairs of IR spectra of water condensed on SWNTs with and without *n*-nonane blocking of the interior sites. *n*-Nonane was condensed on the nanotubes at 123 K and then the sample was heated to 283 K for 15 min before cooling back to 123 K. Other experiments[46] have shown that this results in *n*-nonane occupancy of the interior nanotube sites. Water was then condensed on the sample at 123 K, following by heating to 183 K and cooling to 123 K for IR measurements. Control water adsorption experiments without prior *n*-nonane adsorption were carried out. Figure 3 shows results for the fourth, fifth, and sixth annealing cycles for experiments with and without *n*-nonane blocking of the interior nanotube sites. It is clear that the 3507 $cm^{-1}$ mode is only observed in the absence of *n*-nonane blocking of the internal SWNT sites.

## Results and Discussion

**A. Experimental Results.** Figure 1, spectrum a, shows the infrared spectrum in the OH stretching region following condensation of $H_2O$ at 123 K on the outer geometric surface of the nanotubes. The 3693 $cm^{-1}$ mode corresponds to the free OH groups dangling at the surface of the amorphous ice. These groups disappear upon annealing due to surface reconstruction. Spectra b−f show the consecutive changes that occur as programmed heating to 183 K, followed by quenching to 123 K, occurs (both at 1 K/s rate). The annealing enhances water

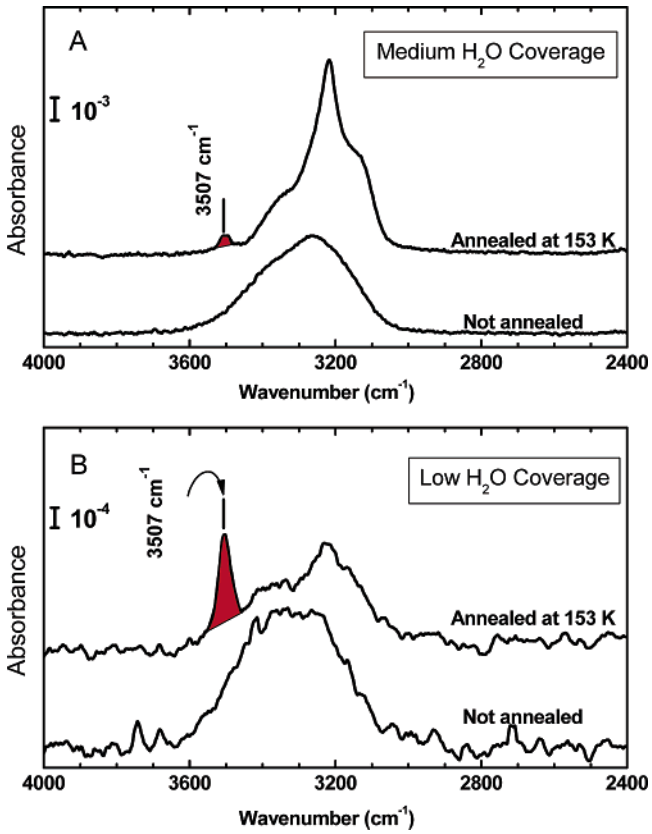


***Figure 2.*** Appearance of the 3507 $cm^{-1}$ OH stretching mode following diffusion of $H_2O$ into the nanotube interior at medium (A) and low (B) coverages.

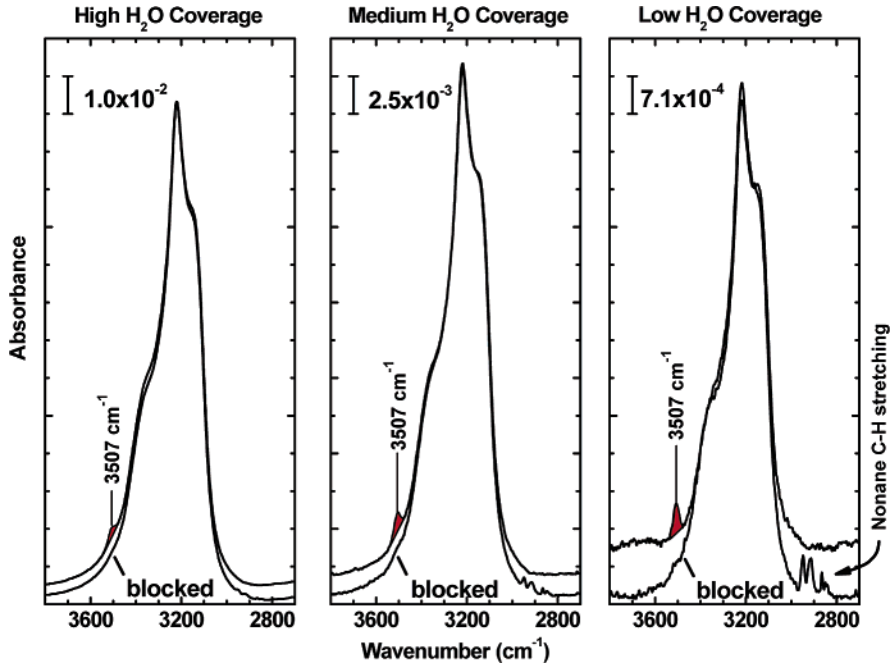


***Figure 3.*** Blocking of the nanotube interior by *n*-nonane preadsorption. The absorbance scale for the middle and right spectra are 1/4 and 1/14 of the scale in the spectra on the left-hand side.

mobility, resulting in $H_2O$ diffusion into the nanotube interior as well as water desorption into vacuum, decreasing the overall amount of condensed water. The development of a high-frequency isolated OH vibrational mode at 3507 $cm^{-1}$ was observed in addition to associated OH features in the 3000−3450 $cm^{-1}$ region.

Figure 2 shows the IR spectra for water condensed at medium and very low $H_2O$ coverages on SWNTs measured before and after the first annealing cycle. In both cases we observe the appearance of a relatively sharp 3507 $cm^{-1}$ mode after annealing. The change of the spectra in the 3000−3600 $cm^{-1}$ range, measured for the medium $H_2O$ coverage (Figure 2A), indicates that water, initially condensed in an amorphous phase on the outer surface of the SWNTs, crystallizes upon annealing. Figure 2B shows that the 3507 $cm^{-1}$ mode is not present in the spectra of condensed water before annealing. This indicates that the 3507 $cm^{-1}$ mode originates from a structure that appears only at temperatures when water molecules possess higher surface mobility and can diffuse in the nanotube interior.

The assignment of the 3507 $cm^{-1}$ mode to internally bound $H_2O$ is based on the effect of n-nonane blocking of the nanotube interior when it is adsorbed below 283 K. At this temperature *n*-nonane is trapped in the nanotube and prevents water from diffusing into the nanotube interior.[46] Figure 3 demonstrates that *n*-nonane blocking almost completely eliminates the mode at 3507 $cm^{-1}$. This clearly shows that the 3507 $cm^{-1}$ mode originates from the water phase confined inside nanotubes. $D_2O$ was employed to verify the observation of the singular OH stretching mode; an analogous mode was observed at 2595 $cm^{-1}$.

The vibrational spectroscopy of condensed water indicates that the higher the degree of involvement of a water molecule into the hydrogen-bond network, the lower the frequency of the OH-stretching modes.[50,51] In the gas-phase spectrum, unbound $H_2O$ molecules exhibit antisymmetric $\nu_3$ and symmetric $\nu_1$ stretching modes at 3756 and 3657 $cm^{-1}$, respectively.[50] A high-frequency free OH stretching mode at 3693 $cm^{-1}$ was observed by us (Figure 1) for dangling hydrogen atoms on the surface of ice nanocrystals at low temperatures and has been reported by others.[52] This mode disappears as the ice nanocrystals are annealed above 140 K due to reconstruction on the ice surface that is accompanied by the formation of strained surface hydrogen bonds.[26] The OH modes of water molecules are red-shifted when the molecule is entrapped in a matrix and does not participate in H-bonding at all or participates only as a proton acceptor to form a hydrogen bond.[24,50] For a proton donor water molecule, the stretching frequency of the OH bond involved in the H-bond network is much more strongly red-shifted relative to the group not involved in the H-bond.[24,50]

One might imagine that the 3507 $cm^{-1}$ mode observed inside nanotubes is caused by OH groups not directly hydrogen bonded but highly red-shifted by the confining environment. This would require a large red-shift of between 150 and 250 $cm^{-1}$ from the free-OH stretching frequency. It is known that molecules confined inside SWNTs exhibit small red-shifts[34,35,43] and that the interaction of the benzene $\pi$-electron cloud with the OH group of a water molecule in a cluster produces a red-shifted mode in the 3636−3657 $cm^{-1}$ range.[24] We have computed the red-shift for a single $H_2O$ inside a (10, 10) SWNT using the VASP[53−56] ab initio density functional theory (DFT) package. Details of the calculations are given in the Supporting Information. The maximum calculated shift is 30 $cm^{-1}$. We therefore conclude that only hydrogen-bonding could cause the red-shift of the free OH frequency down to 3507 $cm^{-1}$, thereby excluding

(50) Scherer, J. R. In *Advances in Infrared and Raman Spectroscopy*; Clark, R. J. H., Hester, R. E., Eds.; Heyden: London, New York, 1975; Vol. 5, p 149.
(51) Nauta, K.; Miller, R. E. *Science* **2000**, *287*, 293.
(52) Hernandez, J.; Uras, N.; Devlin, J. P. *J. Chem. Phys.* **1998**, *108*, 4525.
(53) Kresse, G.; Furthmueller, J. *Phys. Rev. B.* **1996**, *54*, 11169.
(54) Kresse, G.; Furthmueller, J. *Comput. Mat. Sci.* **1996**, *6*, 15.
(55) Kresse, G.; Hafner, J. *Phys. Rev. B.* **1993**, *47*, 558.
(56) Kresse, G.; Hafner, J. *Phys. Rev. B.* **1994**, *49*, 14251.

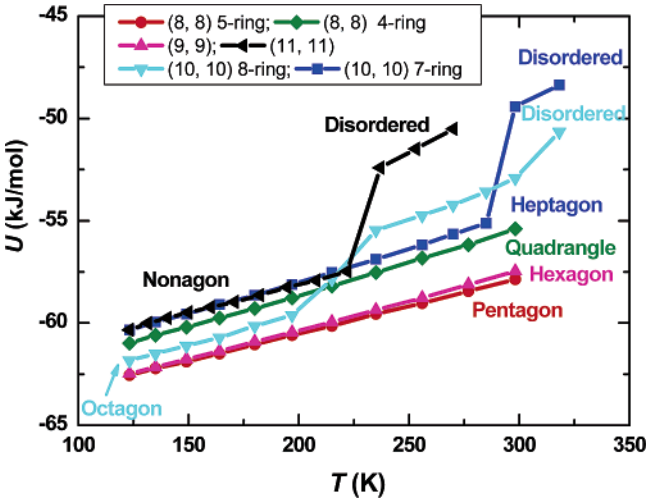


***Figure 4.*** Average energy for water confined in (8, 8), (9, 9), (10, 10), and (11, 11) SWNTs at temperatures ranging from 123 to 318 K from parallel tempering NVT Monte Carlo simulations.

interactions of OH groups with the nanotube interior as being the cause of the 3507 $cm^{-1}$ mode.

**B. Theoretical Results.** We have performed classical molecular simulations for water confined in SWNTs. We have also carried out quantum mechanical DFT calculations for water in ring structures in vacuum and inside a SWNT. Details of the simulations are given in the Supporting Information.

Classical molecular simulations were used to identify structural, energetic, and vibrational properties of water in SWNTs and in the bulk phase at low temperatures. Grand canonical Monte Carlo (GCMC) simulations[57] (Figure S1) were used to efficiently fill nanotubes with water at room temperature. We then performed parallel tempering Monte Carlo simulations[58] in the NVT ensemble over the temperature range from 123 to 298 K [270 and 318 K for (10, 10) and (11, 11) nanotubes, respectively] to identify equilibrium structures at low temperatures. The average energies for water confined in (8, 8), (9, 9), (10, 10), and (11, 11) SWNTs are shown in Figure 4. At low temperatures water forms stacked ring structures in all of the nanotubes considered. See, for example, the water structure in a (10, 10) nanotube shown in Figure 5. The number of water molecules in a ring depends primarily on the diameter of the nanotube. However, the (8, 8) and (10, 10) nanotubes can support different polymorphs. Five- and four-membered rings are observed in the (8, 8) nanotube, while the (10, 10) nanotube can have both eight- and seven-membered rings, as shown in Figure 4. Order-to-disorder structural transitions, indicated by rapid rises in the potential energy with temperature (Figure 4), occur for water confined in (10, 10) and (11, 11) SWNTs; the water remains well-ordered in the smaller diameter nanotubes, even at 298 K. The nanotubes were filled at room temperature for computational efficiency. We have carried out an adsorption isotherm at 183 K for the (10, 10) SWNT to verify that the same structure is ultimately obtained through GCMC simulations as was found from the parallel tempering simulations (see Figure S2). The same stacked ring structures were obtained in the 183 K GCMC simulations, but at a dramatically higher computational cost, as approach to equilibrium is very slow at that temperature.

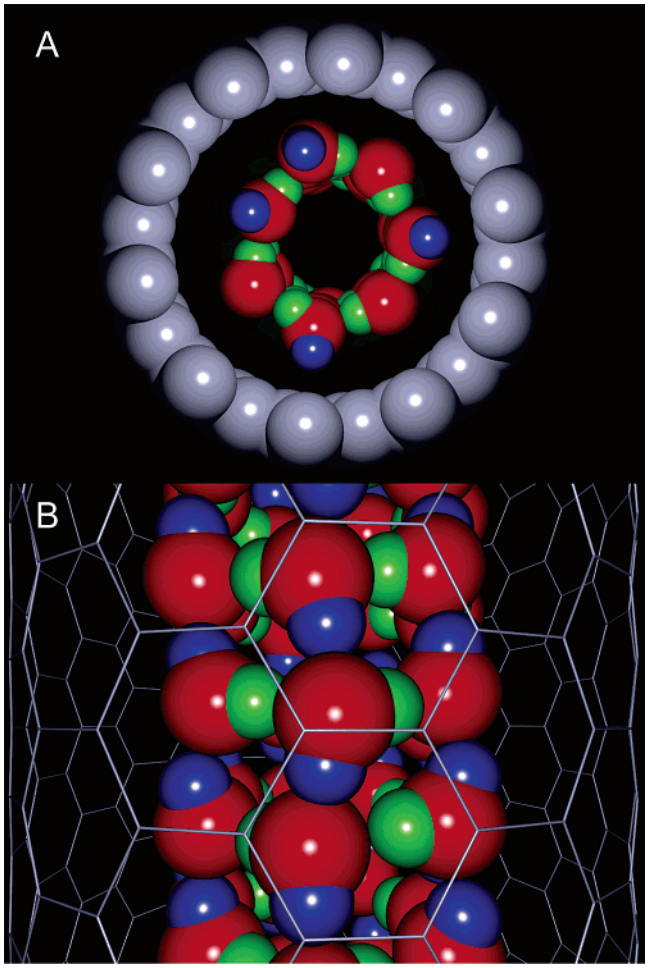


***Figure 5.*** Snapshot from a molecular simulation of water adsorbed inside a (10, 10) SWNT at 123 K forming heptagon rings: (A) end view and (B) side view. Red spheres represent oxygen atoms, blue spheres are hydrogens that are hydrogen-bonded to adjacent rings (inter-ring), and green spheres are hydrogens involved in intra-ring hydrogen bonds. The lines in part B represent the carbon−carbon bonds of the SWNT.

The GCMC simulations at both high and low temperatures and those of Striolo et al.[59] indicate that partial filling of the nanotubes with water is not likely (see Figures S1 and S2). The isotherms indicate an abrupt transition from an empty nanotube to a filled nanotube, consisting of either stacked rings or amorphous water. The 183 K isotherm indicates that both seven- and eight-membered rings could be observed over the range of water vapor pressures likely to be encountered in the experiments. The number of free OH groups for water adsorbed in the nanotubes is not expected to be significant, given the complete filling observed for all nanotubes studied in this work.

The stacked ring structures observed in the nanotubes at low temperatures result in fully hydrogen-bonded water networks. A snapshot of $H_2O$ in a (10, 10) nanotube at 123 K is shown in Figure 5. Figure 5A is an end-on view of the water in the nanotube, clearly showing the heptagon ring structure. The ring structures produce intra- and inter-ring hydrogen bonds. The

(57) Allen, M. P.; Tildesley, D. J. *Computer Simulation of Liquids*; Oxford University Press: New York, 1987.
(58) Frenkel, D.; Smit, B. *Understanding Molecular Simulation: From Algorithms to Applications;* Academic Press: San Diego, CA, 2002.
(59) Striolo, A.; Chialvo, A. A.; Gubbins, K. E.; Cummings, P. T. *J. Chem. Phys.* **2005**, *122*, 234712.

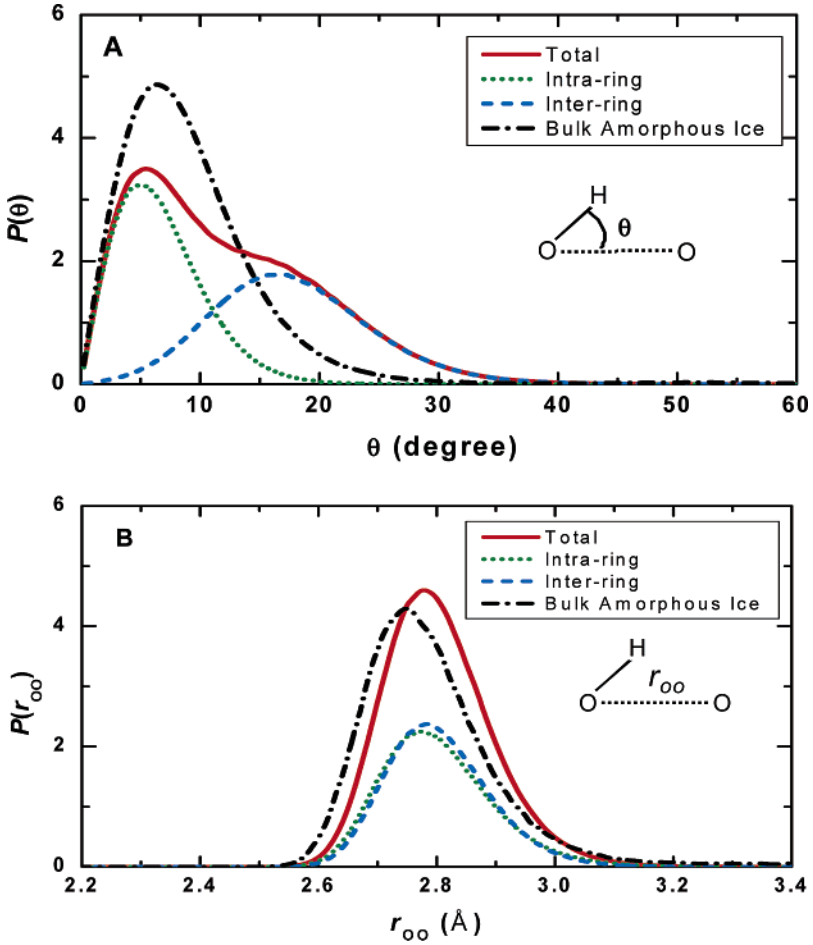


***Figure 6.*** Characteristics of hydrogen bonding in amorphous ice and $H_2O$ forming heptagonal rings inside a (10, 10) SWNT computed from molecular simulations. (A) Hydrogen bond angle (O−OH) distribution computed from Monte Carlo simulation for bulk amorphous ice (dashed−dotted black line) and for $H_2O$ in a (10, 10) SWNT (solid red line). The intra-ring hydrogen bond angles are plotted as the dotted green line, the inter-ring hydrogen bond angles are represented by the dashed blue line, and the red line is the sum of the green and blue lines. The inset shows the definition of the O−OH angle $\theta$. (B) Oxygen−oxygen distance, $r_{OO}$, distribution computed from Monte Carlo simulation for bulk amorphous ice (dashed−dotted black line) and for $H_2O$ in a (10, 10) SWNT (solid red line). The intra-ring O−O distances are plotted as the dotted green line, the inter-ring O−O distances are represented by the dashed blue line, and the red line is the sum of the green and blue lines. The inset shows the definition of the O−O distance $r_{OO}$.

stacked ring structure can be seen in Figure 5B. The oxygen atoms in $H_2O$ are shown in red, the hydrogens participating in intra-ring hydrogen bonds are shown in green, and the inter-ring hydrogen-bonded hydrogens are blue.

The intra-ring hydrogen bonds are bulk-like while most of the inter-ring hydrogen bonds are relatively weak, having a distorted geometry that gives rise to a distinct OH stretching mode. This is illustrated in Figure 6A, using the results of $H_2O$ confined in a (10, 10) SWNT as an example; the distribution of hydrogen-bond angles, measured as the O−OH angle, $\theta$, are reported for bulk amorphous ice and heptagonal ring structured $H_2O$ inside a (10, 10) SWNT, both at 123 K. The probability density for amorphous ice (black line) has a single maximum at $\theta \approx 6°$, whereas $H_2O$ inside a (10, 10) nanotube (red line) has a distribution of hydrogen bond angles that exhibits a maximum at $\theta \approx 5°$ and a shoulder at higher angles. We have analyzed the inter- and intra-ring hydrogen bonds separately and found that the intra-ring hydrogen bond angles (dotted green line) are similar to those of bulk amorphous ice. However, the inter-ring hydrogen bond angles (blue dashed line) are very different from the bulk. The probability density $P(\theta)$ for inter-ring hydrogen bond angles has a Gaussian shape, with a maximum at about 17°. The unusually large hydrogen-bond angles are caused by $H_2O$ confinement in the nanotube.

We have analyzed the distribution of oxygen−oxygen distances, $r_{OO}$, as a surrogate for the hydrogen-bond distances, for bulk and confined $H_2O$ at 123 K. The probability densities, $P(r_{OO})$, for bulk amorphous ice and for $H_2O$ inside a (10, 10) SWNT are plotted in Figure 6B and are seen to be very similar.

We have calculated IR spectra for bulk amorphous ice and water in different nanotubes from classical molecular dynamics (MD) simulations with a flexible water potential.[60] Flexible water potentials have been used previously to compute IR spectra of bulk and confined water from MD simulations.[16] The results of our calculations are plotted in Figures 7 and 8. All of the calculated spectra for water in different nanotubes are qualitatively similar and exhibit two distinct modes, as seen in Figure 7. The low-frequency and the high-frequency modes are due to intra-ring and inter-ring O−H stretching, respectively, as will be demonstrated below. The spectrum of bulk amorphous ice (Figure 8) is much broader than the spectra for water inside nanotubes; the bulk modes are also shifted to lower frequencies. We note that the intensities calculated from classical MD do

(60) Praprotnik, M.; Janezic, D.; Mavri, J. *J. Phys. Chem. A.* **2004**, *108*, 11056.

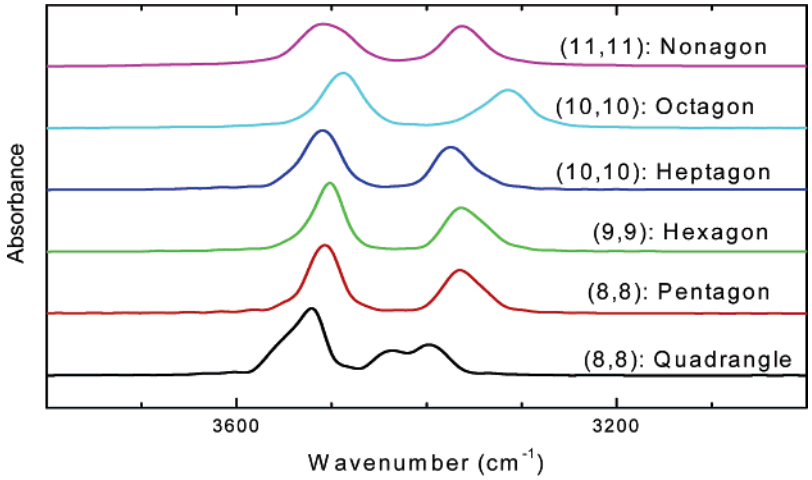


***Figure 7.*** IR spectra for confined water in (8, 8), (9, 9), (10, 10), and (11, 11) SWNTs computed from MD simulations.

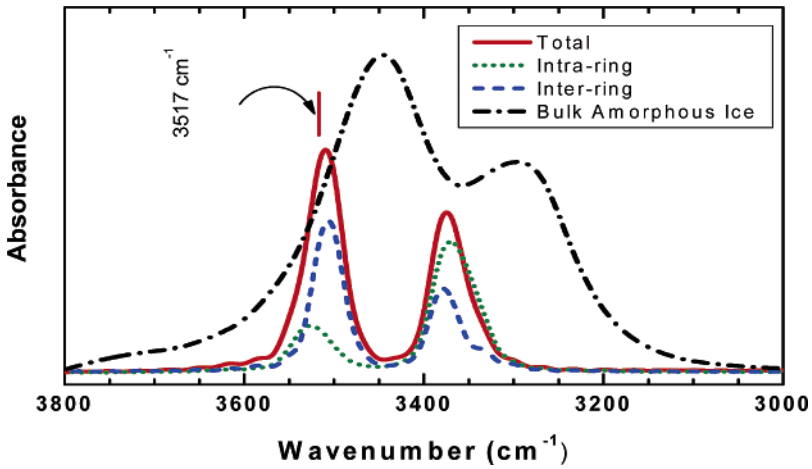


***Figure 8.*** Vibrational spectra computed from molecular dynamics with a flexible water potential. The IR spectra for bulk amorphous ice is plotted as the dashed−dotted black line and the solid red line is for heptagonal water rings in a (10, 10) SWNT. Note the presence of a 3517 $cm^{-1}$ mode, in good agreement with the experimentally observed 3507 $cm^{-1}$ mode frequency. The IR spectrum computed for intra-ring OH stretching is plotted as the dotted green line and the inter-ring spectrum is the dashed blue line. Note that sum of the green and blue lines is not equal to the total spectrum (red line) because of cross correlations.

not capture the enhancement due to hydrogen bonding; however, the frequency distribution is expected to be qualitatively accurate.

We have computed the IR spectrum for intra-ring O−H and for inter-ring O−H stretching separately. The results are presented in Figure 8. The dashed−dotted black line is the spectrum of amorphous ice at 123 K and is in qualitative agreement with the spectrum for the nonannealed case in Figure 2. The solid red line in Figure 8 is the total IR spectrum for $H_2O$ inside a (10, 10) SWNT at 123 K. Two distinct modes are observed, one with a frequency of about 3370 $cm^{-1}$, which lies in the range of bulk hydrogen-bonded OH groups. The other mode is at about 3517 $cm^{-1}$, which corresponds closely with the experimentally observed mode at 3507 $cm^{-1}$. The mode at 3517 $cm^{-1}$ is almost entirely due to inter-ring OH stretching (dashed blue line). Similar results are observed for water adsorbed in a (8, 8), (9, 9), and (11, 11) SWNT and in different sizes of rings, both for the IR spectra (see Figure 7) and the bond angle distributions (see Figures S3 and S4).

We have also computed vibrational frequencies and intensities for water in stacked rings, both inside nanotubes and isolated, from ab initio periodic DFT methods. We have used both the VASP[53−56] and PWscf[61] packages. The DFT calculations confirm the features observed in the classical simulations. The IR spectrum for water in a stacked five-membered ring structure, as in the (8, 8) SWNT, is plotted in Figure 9. The spectrum has been Lorentz broadened by 5 $cm^{-1}$. The low-frequency mode at 3174 $cm^{-1}$ is due to intra-ring hydrogen bonding, while the higher frequency mode at 3555 $cm^{-1}$ is from OH groups involved in weaker inter-ring hydrogen bonds. These two modes are in agreement with the modes observed from classical MD simulations in Figures 7 and 8. Note that the DFT calculations are not expected to give frequencies that agree quantitatively with experiments. However, DFT can capture the enhancement of intensity for the stronger hydrogen-bonded species (intra-ring modes), which the MD simulations cannot. The intensity of the lower frequency mode is about twice that of the higher frequency mode. This intensity enhancement is expected to be qualitatively, but not quantitatively, correct.

The low-frequency modes in the experimental spectra for water inside nanotubes are very broad (see Figures 1−3), while our simulated spectra have relatively sharp low-frequency peaks (Figures 7−9). Much of the experimental broadening can be attributed to amorphous ice on the external surface of the sample.

(61) Baroni, S.; Corso, A. D.; Gironcoli, S. d.; Giannozzi, P. http://www.pwscf.org.

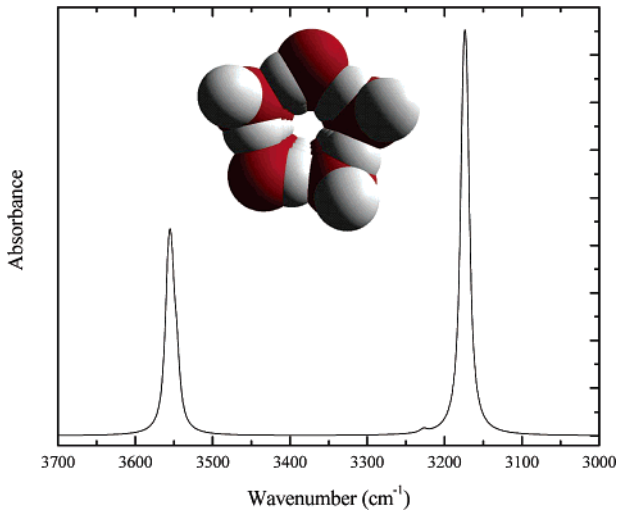


***Figure 9.*** IR spectrum for a pentagonal ring ice structure computed from the PWscf package.[61] The feature at 3555 $cm^{-1}$ is due to inter-ring O−H stretching, while the mode at 3174 $cm^{-1}$ is due to intra-ring O−H stretching. A Lorentz broadening of 5 $cm^{-1}$ has been applied to the spectrum.

However, the low-frequency mode in the spectra at low coverage (Figure 1) is also very broad. Furthermore, the intensity of these modes appears to be attenuated. There are two reasons for the apparent discrepancy between simulations and experiments. (1) The low-frequency (intra-ring) modes are inhomogeneously broadened because of the distribution of nanotube diameters in the experimental sample.[62] Both classical (see Figure 7) and quantum simulations confirm that the low-frequency modes are sensitive to the nanotube diameter while the high-frequency inter-ring modes are relatively insensitive to the diameter of the nanotube. (2) The nanotube bundles are predominantly aligned with their axes parallel to the plane of the tungsten grid, as observed from SEM images, and are therefore perpendicular to the IR beam. This geometric arrangement constrains virtually all of the inter-ring O−H bonds to be perpendicular to the incident IR beam, while a substantial fraction of the intra-ring O−H bonds must be aligned nearly parallel to the IR beam. The geometry of the nanotube sample would therefore attenuate the low-frequency intra-ring mode because any bonds aligned nearly parallel to the IR beam would not add any intensity to the spectrum.

(62) Rinzler, A. G.; Liu, J.; Dai, H.; Nikolaey, P.; Huffman, C. B.; Rodriguez-Macias, F. J.; Boul, P. J.; Lu, A. H.; Heymann, D.; Colbert, D. T.; Lee, R. S.; Fischer, J. E.; Rao, A. M.; Eklund, P. C.; Smalley, R. E. *Appl. Phys. A.* **1998**, *67*, 29.

## Summary

We have found that $H_2O$ molecules confined inside of SWNTs form ring structures that involve hydrogen bonds of two types. Hydrogen bonds within the ring structure exhibit frequencies like those found in bulk $H_2O$ and O−OH angles of near 5°. Hydrogen bonds formed between neighboring rings exhibit an unusual stretching frequency at 3507 $cm^{-1}$ and are associated with larger O−OH angles near 17°. The strained angles and unusual IR mode are a direct result of the confinement-induced stacked ring structures, which would not be stable in the bulk. It is possible that water in other confined environments will exhibit similar distinct stretching frequencies, showing that IR spectroscopy, coupled with atomistic modeling, is proving to be a powerful tool for probing the structure and energetics of confined water.

**Acknowledgment.** We gratefully acknowledge the Army Research Office for the support of this work. We also thank Prof. K. D. Jordan for useful discussions of the results of this work.

**Supporting Information Available:** Computational methods and additional computational results. Coordinates for water in nanotubes from simulation snapshots. This material is available free of charge via the Internet at http://pubs.acs.org.

JA057856U